A POWER RESOLUTION FOR COST EFFECTIVE COMPENSATION AND HARMONIC SOURCE DETECTION IN SMART POWER GRIDS

Murat Erhan BALCI[1], Mehmet Hakan HOCAOGLU [2]

[1]Dept. of Electrical and Electronics Engineering, Balikesir University, Balıkesir, Turkey
[2] Dept. of Electronics Engineering, Gebze Technical University, Kocaeli, Turkey
mbalci@balikesir.edu.tr, hocaoglu@gtu.edu.tr

Abstract: *It is seen from the preliminary work* [1] *of this paper that in the literature there is a need for a power resolution, which can be utilized for (i) the direct provision of the optimum compensation capacitor's power and (ii) obtaining meaningful information on the detection of the harmonic producing loads. This paper proposed a power resolution that can be used to achieve both goals under nosinusoidal and unbalanced conditions in the smart power grids. First goal is important for cost effective unity power factor compensation including a basic capacitor and an active compensator. The second goal is required for the practical detection of harmonic producing loads by using the demand meters, which are employed to measure the powers for the energy billing of the consumers. The proposed power resolution is based on the separation of load current into orthogonal components as active, reactive, scattered conductance, scattered susceptance, unbalanced conductance and unbalanced susceptance currents, which are all related to the conductance and susceptance parameters of the load. To show that the proposed resolution attains its goals, the simulation and experimental based analysis are presented in this paper.*
Keywords: *Power resolutions, nonsinusoidal and unbalanced systems, compensation, harmonic source detection.*

1. Introduction

By the proliferation of a.c. in the transmission and distribution systems, apparent power was defined as the product of voltage and current rms values to size the system equipment and to be a measure for the system efficiency [1, 2]. Historically, the current of the system was divided into two parts: These are; active current, which transports the net energy from source to the load, and reactive current that is the remaining current component when the active part is subtracted from the total current. According to this resolution, apparent power was expressed as the vector sum of active and reactive powers, which flows due to the active and reactive currents, respectively [3]. The ratio of active and apparent powers is named as the power factor, and be utilized to measure the efficiency of the power systems. In addition, conventionally, classical single-phase apparent power is directly extended to three-phase systems by treating each phase individually [1, 4]. Thus, arithmetic apparent power, which is calculated as the arithmetic sum of each phase's apparent power, and vector apparent power, which is calculated as the vector sum of total active and total reactive powers of the system, were constituted for the three-phase systems.

Nevertheless, due to the fact that the classical apparent power and its resolution are defined under sinusoidal and balanced conditions, they did not attain their goals in the case of nonsinusoidal and/or unbalanced conditions. Consequently, a number of apparent power definitions and their resolutions have been proposed for nonsinusoidal single-phase [3, 5-7] and nonsinusoidal & unbalanced three-phase systems [1, 4] to fulfil the gap left out in the classical apparent power concept. However, it is seen from the preliminary work [1] of this paper that in the literature there is a need for a power resolution, which can be utilized for (i) the direct provision of the optimum compensation capacitor's power and (ii) obtaining meaningful information on the detection of the harmonic producing loads. First goal is important for cost effective unity power factor compensation including a basic capacitor and an active compensator. The second goal is useful for the practical detection of harmonic producing loads by using the demand meters, which are employed to measure the powers for the energy billing of the consumers.

As a result, in this paper, for unbalanced nonsinusoidal three-phase and three-line systems, a power resolution is proposed by considering the above mentioned two goals. It should be reminded that the single-phase case of the proposed resolution is interpreted and analysed for compensation in [6, 7]. In addition, this study is partly presented in [8, 9].

Received on: 16.02.2016
Accepted on: 16.05.2016

2. Proposed Power Resolution

In this section, the power resolution proposed in [6, 7] is extended from nonsinusoidal single- phase system to nonsinusoidal and unbalanced three-phase system without neutral line (three-phase and three-line system). Here, it should be underlined that line currents of the three-phase system are nonsinusoidal and unbalanced. However, nonsinusoidal voltages measured in the system has negligible unbalance due to the fact that the considered system has a strong utility side, which means a very low short circuit impedance at fundamental frequency. According to these considerations, in the first step, by expressing line (l=a,b,c) voltages and currents as;

$$\vec{v}(t)=\begin{bmatrix} v_a(t) \\ v_b(t) \\ v_c(t) \end{bmatrix}=\begin{bmatrix} \sum_n \sqrt{2}V_n sin\left(\omega_n t+\theta_{a,n}\right) \\ \sum_n \sqrt{2}V_n sin\left(\omega_n t+\theta_{b,n}\right) \\ \sum_n \sqrt{2}V_n sin\left(\omega_n t+\theta_{c,n}\right) \end{bmatrix},$$
$$\vec{i}(t)=\begin{bmatrix} i_a(t) \\ i_b(t) \\ i_c(t) \end{bmatrix}=\begin{bmatrix} \sum_n \sqrt{2}I_{a,n} sin\left(\omega_n t+\delta_{a,n}\right) \\ \sum_n \sqrt{2}I_{b,n} sin\left(\omega_n t+\delta_{b,n}\right) \\ \sum_n \sqrt{2}I_{c,n} sin\left(\omega_n t+\delta_{c,n}\right) \end{bmatrix} \quad (1)$$

the balanced and unbalanced parts of the line currents can be separated as below:

$$\vec{i}(t)=\vec{i}_B(t)+\vec{i}_u(t) \quad (2)$$

To find the expression of balanced current component ($\vec{i}_B(t)$), the powers ($U_{l,n}$), which are drawn due to the n*th* harmonic line currents in phase with the n*th* harmonic of respective line voltages, and the powers ($Q_{l,n}$), which are drawn due to the n*th* harmonic line currents in quadrature with the n*th* harmonic of respective line voltages, are calculated:

$$U_{l,n}=V_n I_{l,n} cos\left(\theta_{l,n}-\delta_{l,n}\right) \qquad (l=a,b,c) \quad (3)$$
$$Q_{l,n}=V_n I_{l,n} sin\left(\theta_{l,n}-\delta_{l,n}\right) \qquad (l=a,b,c) \quad (4)$$

And then, these powers are shared to each phase equally; thus, fictitious n*th* harmonic balanced active (P_n) and reactive (Q_n) powers are found to be:

$$P_n=\frac{1}{3}\left(U_{a,n}+U_{b,n}+U_{c,n}\right) \quad (5)$$
$$Q_n=\frac{1}{3}\left(Q_{a,n}+Q_{b,n}+Q_{c,n}\right) \quad (6)$$

For n*th* harmonic, balanced active and balanced reactive powers, given in (5) and (6), are drawn by the balanced part of n*th* harmonic equivalent impedance of the three-phase load. Thus, for each phase of the load, n*th* harmonic balanced conductance ($G_{B,n}$) and n*th* harmonic balanced susceptance ($B_{B,n}$) can be calculated as;

$$G_{B,n}=\frac{P_n}{V_n^2} \quad (7)$$
$$B_{B,n}=\frac{Q_n}{V_n^2} \quad (8)$$

By using n*th* harmonic balanced conductance and n*th* harmonic balanced susceptance parameters, the balanced current component can be expressed as;

$$\vec{i}_B(t)=\begin{bmatrix} \sum_n \sqrt{2}G_{B,n}V_n sin\left(\omega_n t+\theta_{a,n}\right) \\ \sum_n \sqrt{2}G_{B,n}V_n sin\left(\omega_n t+\theta_{b,n}\right) \\ \sum_n \sqrt{2}G_{B,n}V_n sin\left(\omega_n t+\theta_{c,n}\right) \end{bmatrix}+ \begin{bmatrix} \sum_n \sqrt{2}B_{B,n}V_n sin\left(\omega_n t+\theta_{a,n}-\frac{\pi}{2}\right) \\ \sum_n \sqrt{2}B_{B,n}V_n sin\left(\omega_n t+\theta_{b,n}-\frac{\pi}{2}\right) \\ \sum_n \sqrt{2}B_{B,n}V_n sin\left(\omega_n t+\theta_{c,n}-\frac{\pi}{2}\right) \end{bmatrix} \quad (9)$$

To find an expression for unbalanced current component ($\vec{i}_u(t)$), the n*th* harmonic conductance ($G_{l,n}$) and n*th* harmonic susceptance ($B_{l,n}$) values seen from *l*=a, b and c phases of the load are written as:

$$G_{l,n}=\frac{U_{l,n}}{V_n^2} \quad (10)$$
$$B_{l,n}=\frac{Q_{l,n}}{V_n^2} \quad (11)$$

Thus, for each phase of the load, n*th* harmonic unbalanced conductance ($G_{l,n}^u$) and n*th* harmonic unbalanced susceptance ($B_{l,n}^u$) values can be found as;

$$G_{l,n}^u=G_{l,n}-G_{B,n} \quad (12)$$
$$B_{l,n}^u=B_{l,n}-B_{B,n} \quad (13)$$

By using $G_{l,n}^u$ and $B_{l,n}^u$, the unbalanced current ($\vec{i}_u(t)$) can be divided into two parts as unbalanced in-phase ($\vec{i}_{up}(t)$) and unbalanced quadrature ($\vec{i}_{uq}(t)$) currents, respectively:

$$\vec{i}_u(t)=\vec{i}_{up}(t)+\vec{i}_{uq}(t)$$
$$=\begin{bmatrix}\sum_n\sqrt{2}G^u_{a,n}V_n\sin(\omega_n t+\theta_{a,n})\\ \sum_n\sqrt{2}G^u_{b,n}V_n\sin(\omega_n t+\theta_{b,n})\\ \sum_n\sqrt{2}G^u_{c,n}V_n\sin(\omega_n t+\theta_{c,n})\end{bmatrix}+$$
$$+\begin{bmatrix}\sum_n\sqrt{2}B^u_{a,n}V_n\sin\left(\omega_n t+\theta_{a,n}-\frac{\pi}{2}\right)\\ \sum_n\sqrt{2}B^u_{b,n}V_n\sin\left(\omega_n t+\theta_{b,n}-\frac{\pi}{2}\right)\\ \sum_n\sqrt{2}B^u_{c,n}V_n\sin\left(\omega_n t+\theta_{c,n}-\frac{\pi}{2}\right)\end{bmatrix} \quad (14)$$

In the second step, the balanced current ($\vec{i}_B(t)$) is decomposed into four orthogonal components namely; active, reactive, scattered conductance and scattered susceptance currents by treating each phase individually. The methodology presented in [6, 7] is considered for the decomposition. This is valid due to the fact that voltage has negligible unbalance and the decomposed current part is completely balanced.

Accordingly, for each phase of the load, equivalent conductance (G_e) is calculated as;

$$G_e=\frac{\sum_n P_n}{\sum_n V_n^2} \quad (15)$$

and active current is written in terms of G_e:

$$\vec{i}_{ac}(t)=\begin{bmatrix}\sum_n\sqrt{2}G_eV_n\sin(\omega_n t+\theta_{a,n})\\ \sum_n\sqrt{2}G_eV_n\sin(\omega_n t+\theta_{b,n})\\ \sum_n\sqrt{2}G_eV_n\sin(\omega_n t+\theta_{c,n})\end{bmatrix} \quad (16)$$

And then, for each phase of the load, by calculating n*th* harmonic equivalent susceptance ($B_{e,n}$) as;

$$B_{e,n}=nB_{e,1}=n\frac{1}{Xc_1},\ Xc_1=\sum_n n^2V_n^2\Big/\sum_n nQ_n \quad (17)$$

reactive current can be expressed as:

$$\vec{i}_r(t)=\begin{bmatrix}\sum_n\sqrt{2}B_{e,n}V_n\sin\left(\omega_n t+\theta_{a,n}-\frac{\pi}{2}\right)\\ \sum_n\sqrt{2}B_{e,n}V_n\sin\left(\omega_n t+\theta_{b,n}-\frac{\pi}{2}\right)\\ \sum_n\sqrt{2}B_{e,n}V_n\sin\left(\omega_n t+\theta_{c,n}-\frac{\pi}{2}\right)\end{bmatrix} \quad (18)$$

Sequently, using (16) and (18), the expression of the balanced current is rewritten in terms of active, reactive and scattered ($\vec{i}_s(t)$) currents:

$$\vec{i}_B(t)=\begin{bmatrix}\sum_n\sqrt{2}G_eV_n\sin(\omega_n t+\theta_{a,n})\\ \sum_n\sqrt{2}G_eV_n\sin(\omega_n t+\theta_{b,n})\\ \sum_n\sqrt{2}G_eV_n\sin(\omega_n t+\theta_{c,n})\end{bmatrix}+$$
$$+\begin{bmatrix}\sum_n\sqrt{2}B_{e,n}V_n\sin\left(\omega_n t+\theta_{a,n}-\frac{\pi}{2}\right)\\ \sum_n\sqrt{2}B_{e,n}V_n\sin\left(\omega_n t+\theta_{b,n}-\frac{\pi}{2}\right)\\ \sum_n\sqrt{2}B_{e,n}V_n\sin\left(\omega_n t+\theta_{c,n}-\frac{\pi}{2}\right)\end{bmatrix}+\vec{i}_s(t) \quad (19)$$

By equating the right hand sides of (9) and (19), $\vec{i}_s(t)$ can be expressed as:

$$\vec{i}_s(t)=\begin{bmatrix}\sum_n\sqrt{2}(G_{B,n}-G_e)V_n\sin(\omega_n t+\theta_{a,n})\\ \sum_n\sqrt{2}(G_{B,n}-G_e)V_n\sin(\omega_n t+\theta_{b,n})\\ \sum_n\sqrt{2}(G_{B,n}-G_e)V_n\sin(\omega_n t+\theta_{c,n})\end{bmatrix}+$$
$$+\begin{bmatrix}\sum_n\sqrt{2}(B_{B,n}-B_{e,n})V_n\sin\left(\omega_n t+\theta_{a,n}-\frac{\pi}{2}\right)\\ \sum_n\sqrt{2}(B_{B,n}-B_{e,n})V_n\sin\left(\omega_n t+\theta_{b,n}-\frac{\pi}{2}\right)\\ \sum_n\sqrt{2}(B_{B,n}-B_{e,n})V_n\sin\left(\omega_n t+\theta_{c,n}-\frac{\pi}{2}\right)\end{bmatrix} \quad (20)$$

And lastly, the parts related to conductance and susceptance of $\vec{i}_s(t)$ can be named as scattered conductance current;

$$\vec{i}_{sc}(t)=\begin{bmatrix}\sum_n\sqrt{2}(G_{B,n}-G_e)V_n\sin(\omega_n t+\theta_{a,n})\\ \sum_n\sqrt{2}(G_{B,n}-G_e)V_n\sin(\omega_n t+\theta_{b,n})\\ \sum_n\sqrt{2}(G_{B,n}-G_e)V_n\sin(\omega_n t+\theta_{c,n})\end{bmatrix} \quad (21)$$

and scattered susceptance current;

$$\vec{i}_{ss}(t)=\begin{bmatrix}\sum_n\sqrt{2}(B_{B,n}-B_{e,n})V_n\sin\left(\omega_n t+\theta_{a,n}-\frac{\pi}{2}\right)\\ \sum_n\sqrt{2}(B_{B,n}-B_{e,n})V_n\sin\left(\omega_n t+\theta_{b,n}-\frac{\pi}{2}\right)\\ \sum_n\sqrt{2}(B_{B,n}-B_{e,n})V_n\sin\left(\omega_n t+\theta_{c,n}-\frac{\pi}{2}\right)\end{bmatrix} \quad (22)$$

As a result, the load current can be written as;

$$\vec{i}(t)=\vec{i}_{ac}(t)+\vec{i}_{r}(t)+\vec{i}_{sc}(t)+\vec{i}_{ss}(t)+\vec{i}_{up}(t)+\vec{i}_{uq}(t) \quad (23)$$

By considering the collective rms current expression of the Buchollz's apparent power definition [1, 4, 10], the rms values of the currents placed in (23) can be calculated as;
total current's rms value;

$$I_{\Sigma}=\sqrt{\frac{1}{T}\int_{0}^{T}\left(\vec{i}(t)\right)^{Tr}\cdot\vec{i}(t)dt}=\sqrt{\sum_{l}I_{l}^{2}} \quad (24)$$

active current's rms value,

$$I_{ac}=\sqrt{\frac{1}{T}\int_{0}^{T}\left(\vec{i}_{ac}(t)\right)^{Tr}\cdot\vec{i}_{ac}(t)dt}=\sqrt{3G_{e}^{2}\sum_{n}V_{n}^{2}} \quad (25)$$

reactive current's rms value,

$$I_{r}=\sqrt{\frac{1}{T}\int_{0}^{T}\left(\vec{i}_{r}(t)\right)^{Tr}\cdot\vec{i}_{r}(t)dt}=\sqrt{3\sum_{n}B_{e,n}^{2}V_{n}^{2}} \quad (26)$$

scattered conductance current's rms value,

$$\begin{aligned}I_{sc}&=\sqrt{\frac{1}{T}\int_{0}^{T}\left(\vec{i}_{sc}(t)\right)^{Tr}\cdot\vec{i}_{sc}(t)dt}\\&=\sqrt{3\sum_{n}\left(G_{B,n}-G_{e}\right)^{2}V_{n}^{2}}\end{aligned} \quad (27)$$

scattered susceptance current's rms value,

$$\begin{aligned}I_{ss}&=\sqrt{\frac{1}{T}\int_{0}^{T}\left(\vec{i}_{ss}(t)\right)^{Tr}\cdot\vec{i}_{ss}(t)dt}\\&=\sqrt{3\sum_{n}\left(B_{B,n}-B_{e,n}\right)^{2}V_{n}^{2}}\end{aligned} \quad (28)$$

unbalanced in phase current's rms value,

$$\begin{aligned}I_{up}&=\sqrt{\frac{1}{T}\int_{0}^{T}\left(\vec{i}_{up}(t)\right)^{Tr}\cdot\vec{i}_{up}(t)dt}\\&=\sqrt{\sum_{n}\left[\left(G_{a,n}^{u}\right)^{2}+\left(G_{b,n}^{u}\right)^{2}+\left(G_{c,n}^{u}\right)^{2}\right]V_{n}^{2}}\end{aligned} \quad (29)$$

and unbalanced quadrature current's rms value,

$$\begin{aligned}I_{uq}&=\sqrt{\frac{1}{T}\int_{0}^{T}\left(\vec{i}_{uq}(t)\right)^{Tr}\cdot\vec{i}_{uq}(t)dt}\\&=\sqrt{\sum_{n}\left[\left(B_{a,n}^{u}\right)^{2}+\left(B_{b,n}^{u}\right)^{2}+\left(B_{c,n}^{u}\right)^{2}\right]V_{n}^{2}}\end{aligned} \quad (30)$$

In (24)-(30), the superscript "Tr" denotes transpose of the respected three-phase current vector.
Since n*th* harmonic of conductance based current components are in phase with the n*th* harmonic of voltage and the n*th* harmonic of susceptance based current components are in quadrature with the n*th* harmonic of voltage, all combinations between conductance based currents and susceptance based currents are orthogonal. The orthogonality proofs of the rest combinations of the proposed current components are provided in [8]. Therefore, the collective rms value of the total current can be expressed as the vector sum of the collective rms values of the proposed current components:

$$I_{\Sigma}^{2}=I_{ac}^{2}+I_{r}^{2}+I_{sc}^{2}+I_{ss}^{2}+I_{up}^{2}+I_{uq}^{2} \quad (31)$$

Finally, if both sides of (31) are multiplied by the square of collective voltage rms value ($V_{\Sigma}^{2}=\sum_{l}V_{l}^{2}$), the resolution of Buchollz's apparent power (S) can be obtained as;

$$\begin{aligned}S^{2}&=V_{\Sigma}^{2}I_{\Sigma}^{2}=V_{\Sigma}^{2}I_{ac}^{2}+V_{\Sigma}^{2}I_{r}^{2}+V_{\Sigma}^{2}I_{sc}^{2}+V_{\Sigma}^{2}I_{ss}^{2}+V_{\Sigma}^{2}I_{up}^{2}+V_{\Sigma}^{2}I_{uq}^{2}\\&=P^{2}+Q_{r}^{2}+D_{sc}^{2}+D_{ss}^{2}+D_{up}^{2}+D_{uq}^{2}\end{aligned} \quad (32)$$

In (32), power components are named as active (P), reactive (Q_r), scattered conductance (D_{sc}), scattered susceptance (D_{ss}), unbalanced in phase (D_{up}) and unbalanced quadrature (D_{uq}) powers. Note that for the systems without zero sequence voltages, the apparent powers of Buchollz [1, 10] and IEEE standard 1459 [11] have the same numerical values [12, 13]. Thus, proposed power resolution also decomposes IEEE standard 1459 apparent power.

To point out the novelty of the proposed resolution, here it is compared with Czarnecki's power resolution [14, 15], which is similar to the proposed one:

- The reactive power component of Czarnecki's resolution is divided into two power components, namely; reactive power and scattered susceptance power in the proposed resolution. The reactive power component of the proposed resolution is completely compensated when the power factor is maximized by the balanced three-phase capacitors bank. However, this is not the case for the reactive power component of Czarnecki's resolution.
- And also, the unbalanced power component of Czarnecki's power resolution is decomposed into unbalanced in phase and unbalanced quadrature powers in the proposed resolution:

$$D_{u}^{2}=D_{up}^{2}+D_{uq}^{2}=V_{\Sigma}^{2}\left(I_{up}^{2}+I_{uq}^{2}\right) \quad (33)$$

As a result, in the proposed resolution, all power components are expressed in terms of the conductance and susceptance parameters of the load. This should be useful for cooperative design

and control of different types of harmonic, unbalance and reactive power compensators.

The contributions of the proposed power resolution to frequency-domain power theory are detailed below:

2.1. Providing a Tool for Cost Effective Unity Power Factor Compensation

As mentioned before, the reactive power (Q_r) of the proposed resolution is completely compensated when the power factor is maximized by the balanced three-phase capacitors bank. But, its other nonactive powers (D_{sc}, D_{ss}, D_{up} and D_{uq}) do not have any portions compensable via the balanced capacitors bank. This means that Q_r gives the power of optimum balanced capacitive compensator (S_{pC}), which maximizes the power factor under the nonsinusoidal voltage and current conditions:

$$S_{pC} = Q_r \tag{34}$$

In addition to that, for the cost effective unity power factor compensation scheme including the balanced capacitors bank and an active filter, the power (S_{aC}) of the active filter can practically be sized as the vector sum of D_{sc}, D_{ss}, D_{up} and D_{uq}:

$$S_{aC} = \sqrt{D_{sc}^2 + D_{ss}^2 + D_{up}^2 + D_{uq}^2} \tag{35}$$

For this compensation scheme, according to unity power factor instantaneous compensation strategy [16], the active filter (or compensator) should inject the current ($\vec{i}_{af}(t)$), given in (36), into the system:

$$\vec{i}_{af}(t) = \vec{i}_{sc}(t) + \vec{i}_{ss}(t) + \vec{i}_{up}(t) + \vec{i}_{uq}(t) \tag{36}$$

2.2. Providing a Tool for the Detection of the Harmonic Producing Loads

From the outlines of the proposed power resolution, it can be qualitatively concluded that two power components could be used to detect the harmonic producing loads: These are; scattered conductance power (D_{sc}), which occurs by the difference between *n*th harmonic balanced conductance and equivalent conductance, and scattered susceptance power (D_{ss}), which occurs by the difference between *n*th harmonic balanced susceptance and *n*th harmonic equivalent susceptance. However, D_{ss} is quiet sensitive to the source side's harmonic distortion, thus; its usage for the detection of the harmonic producing loads will be problematic. On the other hand, D_{sc} has the cases underlined below;

- **Sinusoidal Voltage (or Voltage with Negligible *THD*V):** For a linear load under negligible voltage distortion, apparent power is very close to the fundamental harmonic apparent power due to the fact that both voltage and current harmonics have negligible magnitudes. As a result, for the same load-voltage case, D_{sc} has negligible value. On the contrary, for a nonlinear (or harmonic producing) load under the same voltage case, the load's balanced conductances calculated for the harmonics a part from fundamental one have the considerable values due to the fact that the load injects current harmonics, which is extremely higher than the respective voltage harmonics. Therefore, the rms value of the scattered conductance current (I_{sc}) and D_{sc} have considerably high values for the nonlinear load condition.
- **Nonsinusoidal Voltage:** In IEEE standard 519 [17], the maximum permissible value of THD_V is determined as 5% at the bus voltages lower than 69kV, 2.5% at the bus voltages between 69kV and 161kV and 1.5% at the bus voltages higher than 161kV. Thus, according to the same standard, the maximum value of THD_V measured at point of common coupling (pcc) can be assumed as 5%. For the maximum voltage distortion level, a linear load draws very small harmonic currents if there is no any resonance condition in the system. As a result, I_{sc} and D_{sc} of the linear load will be small. For a harmonic producing load under the same voltage distortion level, it is feasible that its current have some harmonic components, which is extremely larger than respective harmonic components of the voltage, in other words it behaves as considerably large conductances for the respective harmonic numbers. Consequently, I_{sc} and D_{sc} drawn by the harmonic producing load will have considerable values under the distorted supply voltage condition.

According to the manners mentioned above, it can be concluded whether the load has a non-harmonic producing characteristic or not.

3. Analysis Results on Reactive Power Compensation

In this section, it will be demonstrated that the proposed resolution can be used as a tool to obtain the power of optimum balanced capacitive compensator, which maximizes power factor under nonsinusoidal conditions. In addition, it will also be pointed out that the unity power factor can be achieved cost effectively by using the combination of the optimum balanced capacitive and active compensators (hybrid compensation). In other words, it will be shown that the power of active compensator in the hybrid compensation scheme could be smaller than used in pure active compensation scheme. The merit of the proposed resolution for the direct implementation of hybrid compensation will be simulated in the system, given in Figure 1. The simulated system consists of four kinds of loads, which are a resistive load supplied with frequency converter, a six-pulse rectifier with resistive load, a six-pulse rectifier with dc motor and an unbalanced inductive load. For the system without compensation (NC), the waveshapes of the line voltages and line currents are given in Figure 2 and Figure 3, respectively.

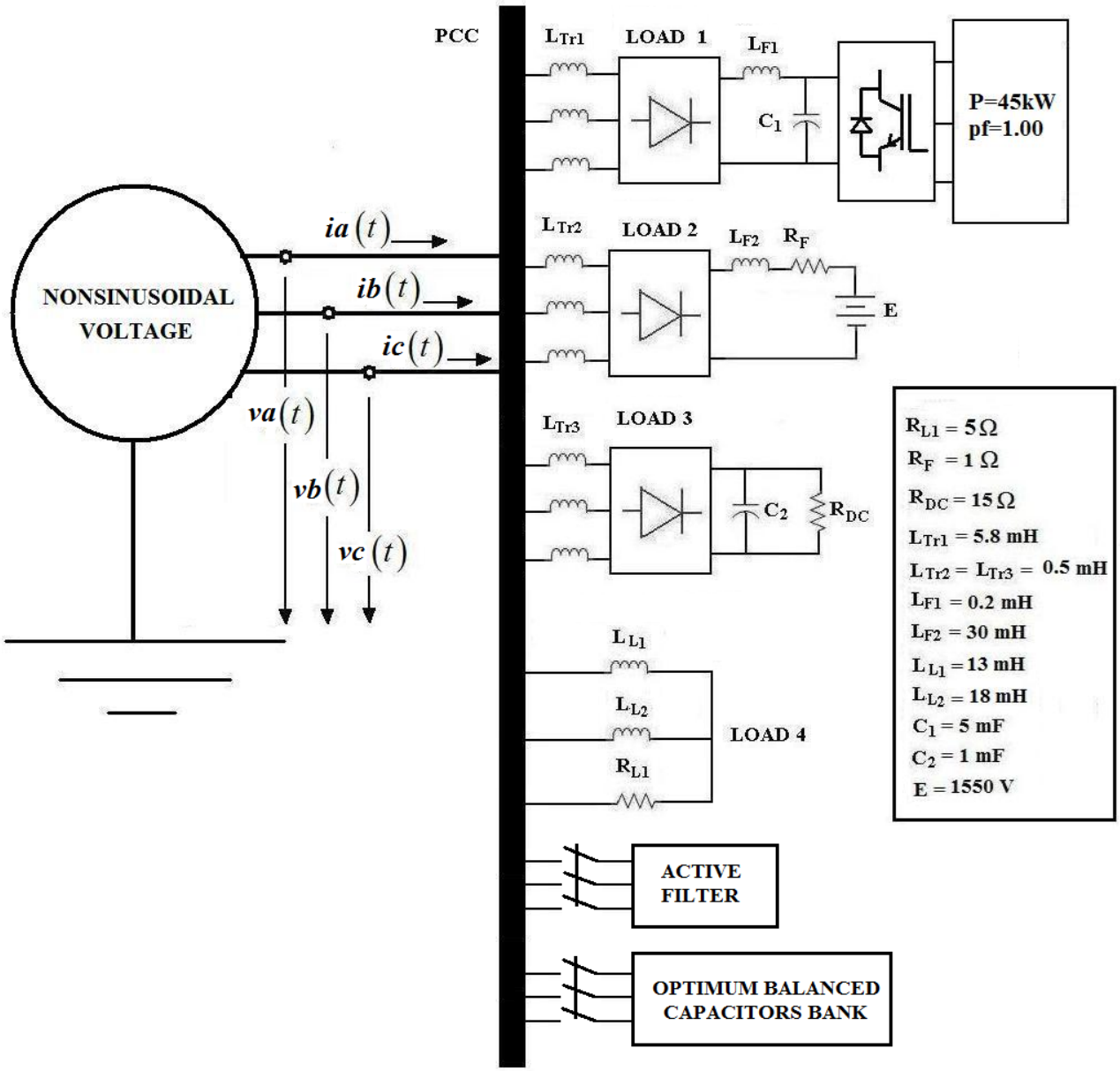

Figure 1. The simulated system considered for the compensation analysis

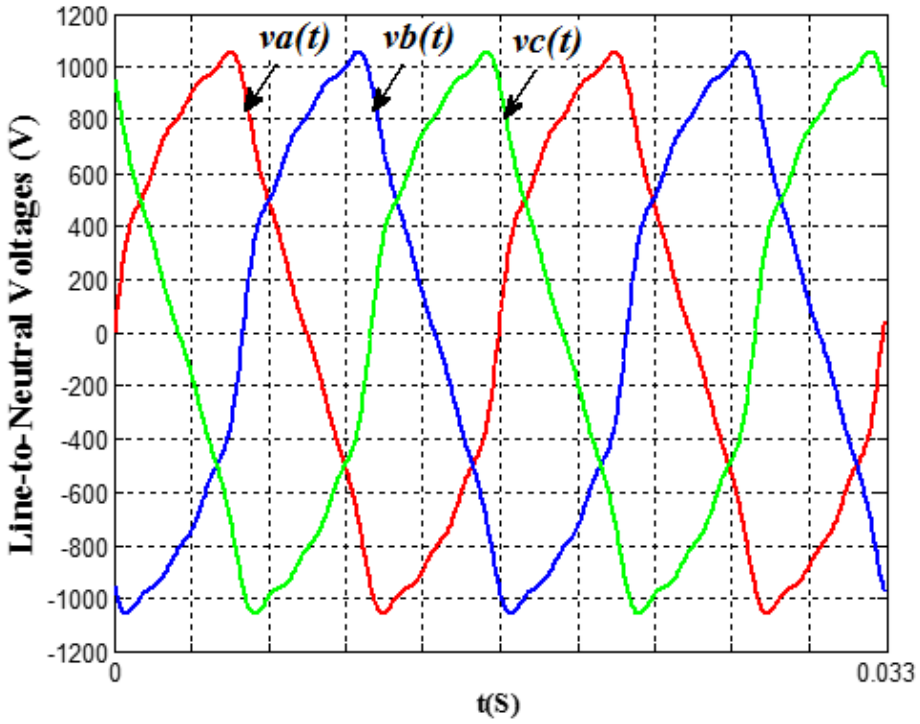

Figure 2. The wave shapes of the line voltages of the simulated system

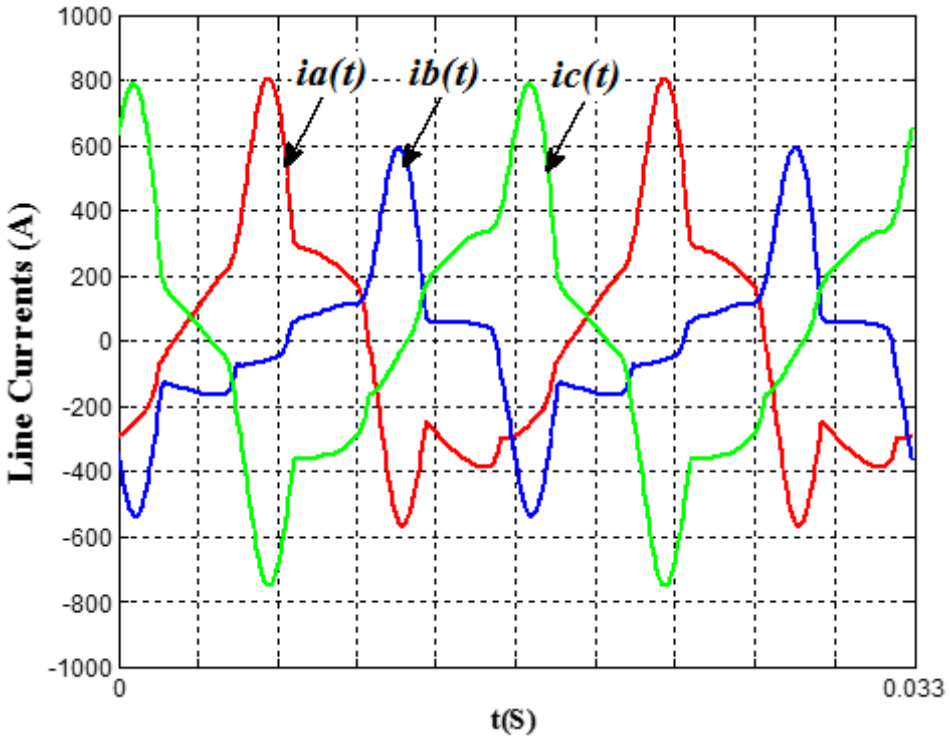

Figure 3. The wave shapes of the line currents of the simulated system without compensation (NC)

Figure 2 shows that line voltages have nonsinusoidal and balanced wave forms, which have 10% of THD_V. The line currents, plotted in Figure 3, have nonsinusoidal wave forms with 42%, 70% and 39% of THD_I, respectively. They are also significantly unbalanced: the ratio between fundamental harmonic negative and fundamental harmonic positive sequence magnitudes of the line currents, I_1^-/I_1^+, is 32.3%.

For the system without compensation (NC), with optimum balanced capacitive compensation (OBC), active compensation (AC) and hybrid compensation (HC), the proposed power components (P, Q_r, D_{sc}, D_{ss}, D_{up} and D_{uq}), apparent power (S), the powers of passive and active compensators (S_{pC} and S_{aC}) and power factor (pf=P/S) are plotted in Figure 4 and Figure 5. It should be noted that optimum balanced capacitive compensator is a star connected three identical capacitors, of which the capacitances can be determined using (17), active compensation is undertaken by unity power factor compensation strategy [16].

Figure 4 and 5 show that for NC case, pf, Q_r and S are 0.756, 0.435pu and 1.00pu. In addition to that, for NC case, vector sum of D_{sc}, D_{ss}, D_{up} and D_{uq} is 0.489pu. For OBC case, Q_r is completely compensated and pf is improved from 0.756 to 0.840 by using star connected three identical capacitors, of which the power (S_{pc}) is 0.435pu. Obviously, all power components except Q_r have the same values for NC and OBC cases. Thus, one can see that Q_r gives the power of optimum balanced capacitive compensator. On the other hand, pf is still smaller than unity for OBC since D_{sc}, D_{ss}, D_{up} and D_{uq} can not be compensated via the balanced capacitive compensator. For AC case, unity power factor is achieved by using only active compensator, of which power (S_{ac}) is equal to 0.654pu, and S is decreased to 0.756pu. For HC case, unity power factor is achieved by using the optimum balanced capacitive compensator, of which power is 0.435pu, and an active compensator, of which power is equal to 0.489pu. Therefore, it can be pointed out that the power of active compensator used in hybrid compensation is 74.7% of active compensator's power calculated for the pure active compensation. In addition, it should also be underlined that for HC case, Q_r and the vector sum of the D_{sc}, D_{ss}, D_{up} and D_{uq} are equal to S_{pC} and S_{aC}, respectively. This means that the proposed resolution can practically be employed as a tool to design the cost effective unity power factor compensator consisting of the basic capacitors and an active compensator.

4. Experimental Analysis on the Detection of Harmonic Producing Loads

In this section, the harmonic producing load detection method based on the proposed power resolution is statistically evaluated by using a real test system, which comprises various types of linear and nonlinear loads. The schematic of the system are depicted in Figure 6. In the schematic, PC processes voltage and current data, and controls the programmable power supply, which generates the desired voltage wave forms. A R-L impedance with X/R=0.5, an induction machine working with the constant speed and constant torque cases under full loading, a dimmer controlled R-L impedance (X/R=0.5 and the triac conduction angles: 90°-270°), a number of computers and a number of compact fluorescent lamps are the load types employed in the test system.

Each one of the loads are supplied with one sinusoidal and one hundred randomly produced different distorted voltages with 5% value of THD_V. For the sinusoidal excitation, voltage and current pairs of the loads are plotted in Figure 7. It is seen from Figure 7 (a) that the current of the R-L impedance load under sinusoidal supply voltage is sinusoidal. Figure 7 (b) and (c) shows that the induction machine draws a current with small amount of THD_I, which is measured as 5%, under sinusoidal supply voltage. On the other hand, the currents of the dimmer controlled R-L impedance, computers and compact fluorescent lamps, of which THD_I values are measured as 50, 185 and 115%, respectively, are seen as highly distorted from Figure 7 (d), (e) and (f).

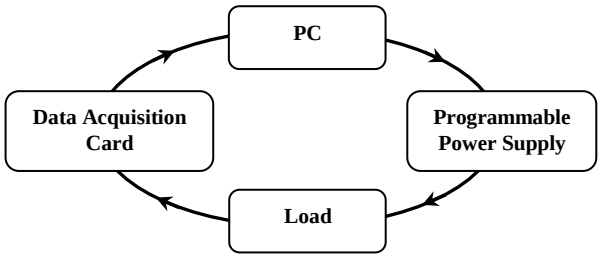

Figure 6. The schematic of the test system used for the harmonic source detection analysis

The normalised values of the powers measured under sinusoidal supply voltage and the histograms of the normalised values of the powers measured under distorted test voltages are presented in Figure 8 and Figure 9, respectively. Figure 8 (a) shows that the R-L impedance draws P and Q_r measured as 0.89 and 0.44 pu, respectively. In addition, D_{sc} and D_{ss} values of the R-L impedance are almost zero under the sinusoidal supply voltage. Figure 8 (a) and (d) point out that for the same load type the P, Q_r and D_{sc} values measured under one hundred distorted test voltages are very close to their measured values under sinusoidal supply voltage. However, under the distorted test voltages, the D_{ss} values drawn by the R-L impedance vary between 0.1 and 0.2 pu. This clearly means that D_{ss} is strongly dependent on the source side distortion.

Figure 8 (b) points out that the induction machine working with constant speed draws P, Q_r, D_{sc} and D_{ss} measured as 0.81, 0.58, 0.03 and 0.04 pu, respectively. It is seen from Figure 8 (b) and (e) that P, Q_r and D_{sc} values measured under the distorted test voltages are around their measured values under sinusoidal supply voltage. However, for the distorted test voltages, D_{ss} varies between 0.1 and 0.2 pu.

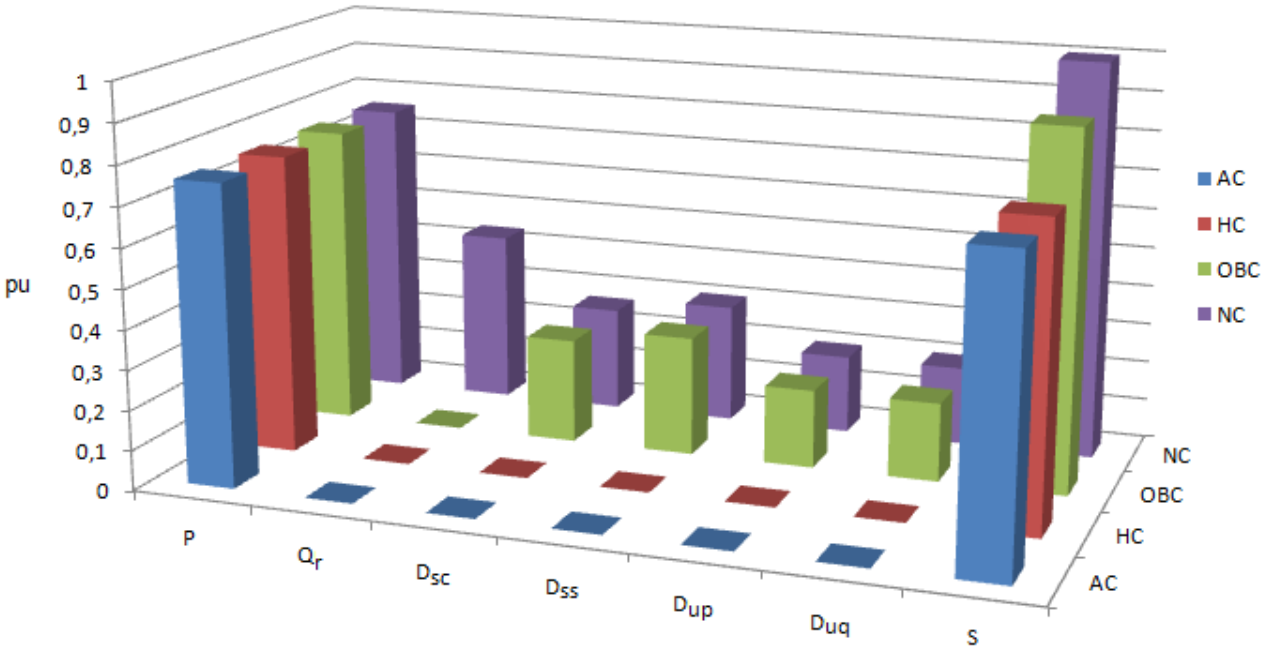

Figure 4. Powers measured at the pcc of the simulated system for the NC, OBC, HC and AC cases

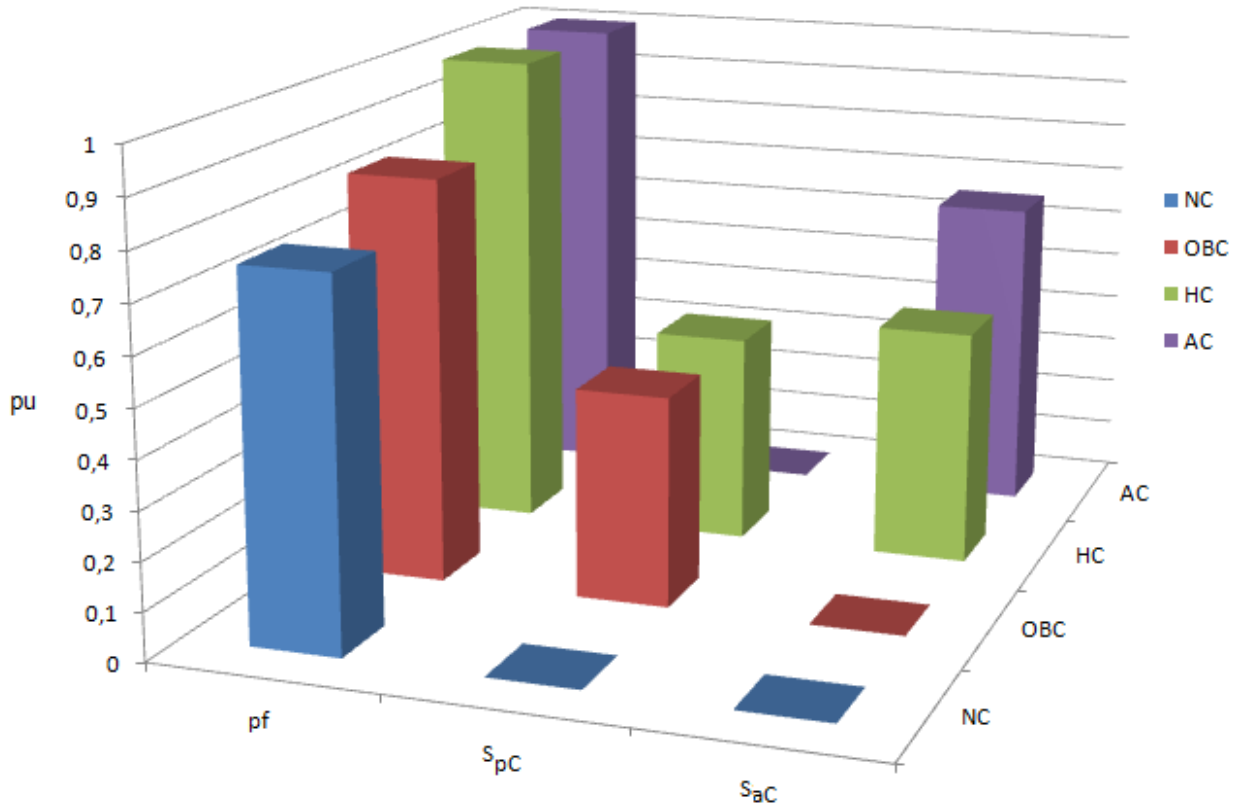

Figure 5. The powers of compensators and power factors for the NC, OBC, HC and AC cases

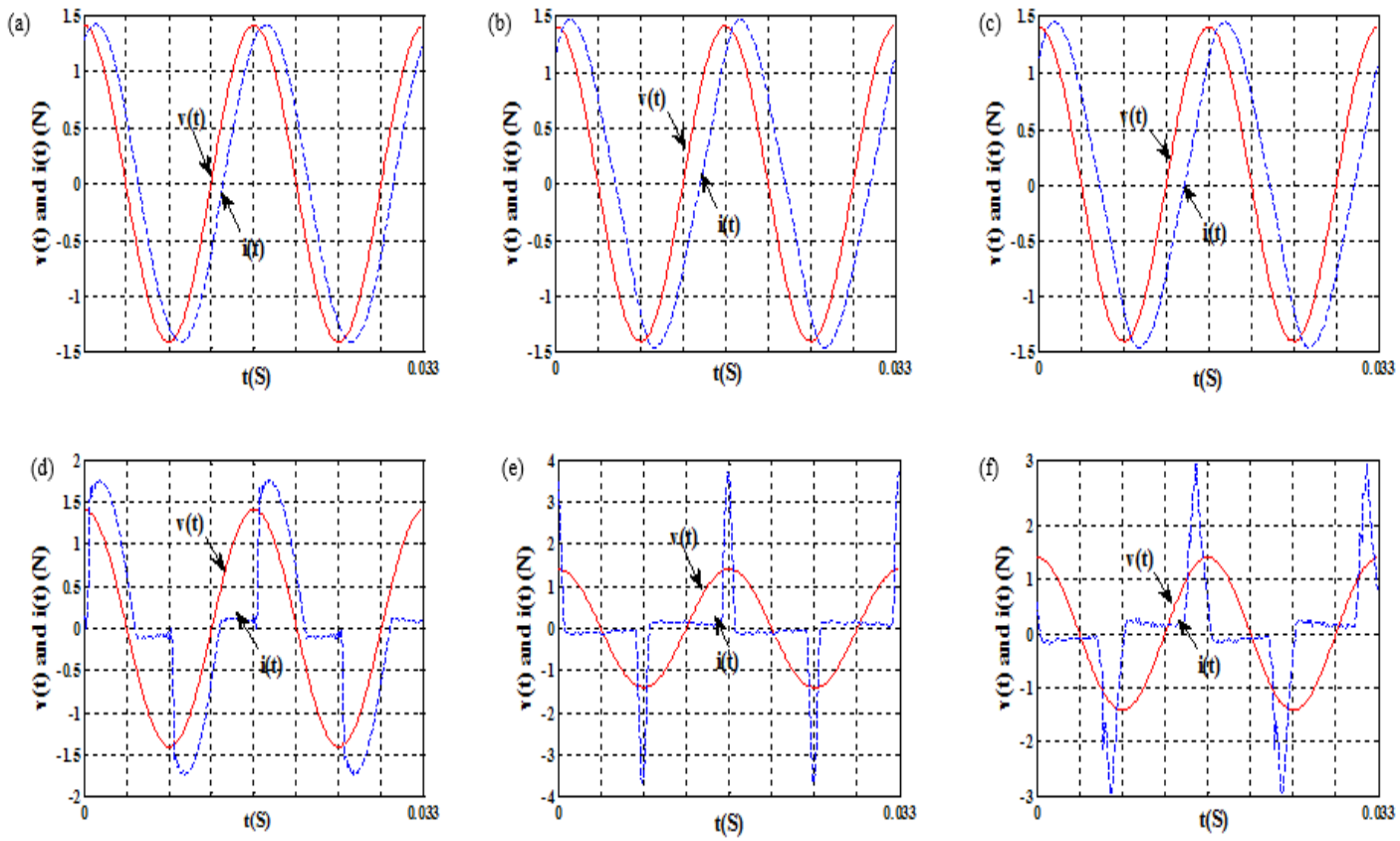

Figure 7. For sinusoidal excitation, the voltage and current pairs of (a) the R-L impedance, (b) the induction machine working with constant speed, (c) the induction machine working with constant torque, (d) the R-L impedance controlled with a dimming circuit, (e) a number of computers and (f) a number of compact fluorescent lamps.

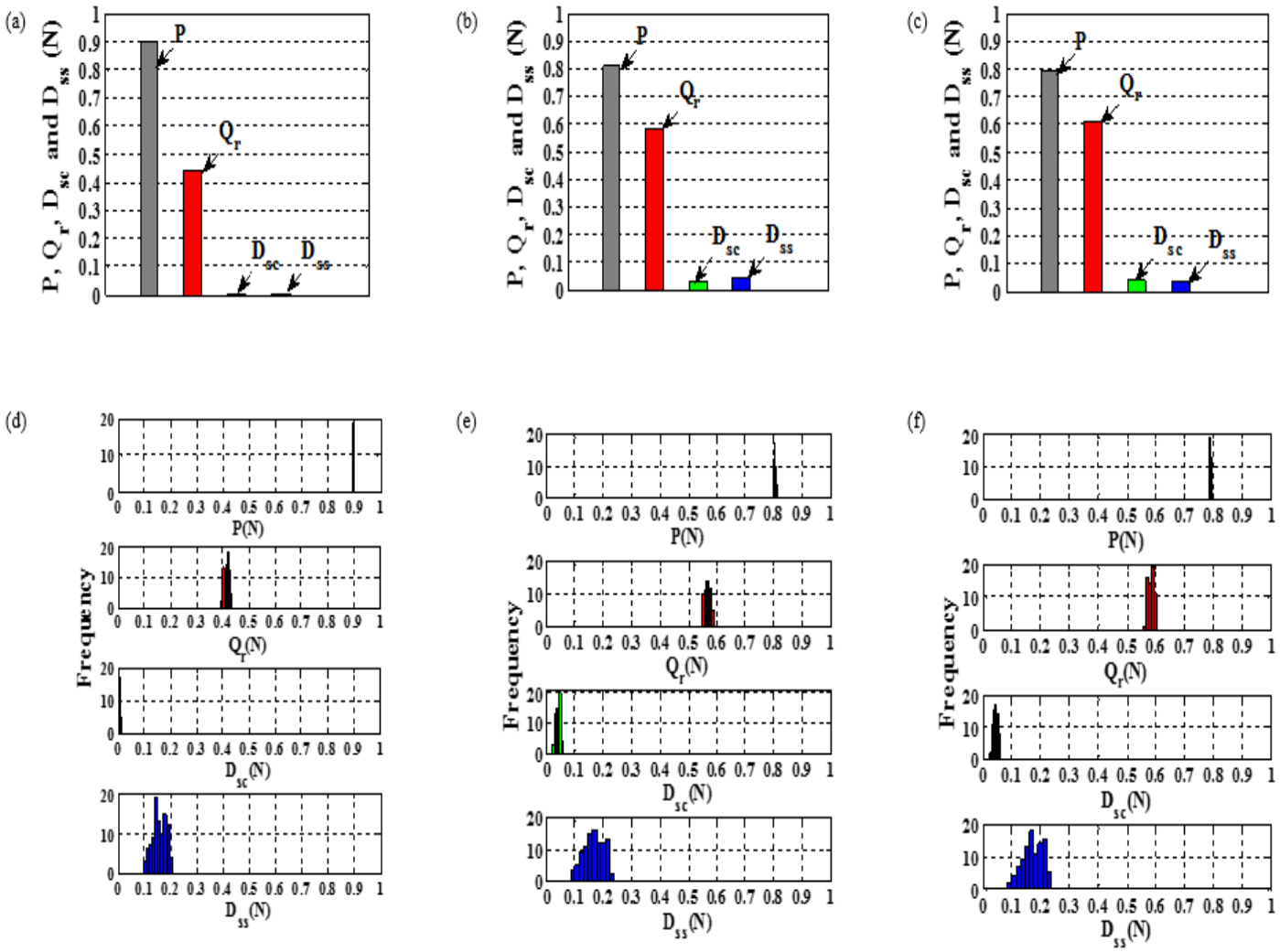

Figure 8. The normalised values of P, Q_r, D_{sc} and D_{ss} measured under sinusoidal supply voltage for (a) a R-L impedance, (b) the constant speed case of an induction machine and (c) the constant torque case of an induction machine, and the histograms of the normalised powers measured under distorted test voltages for (d) a R-L impedance, (e) the constant speed case of an induction machine and (f) constant torque case of an induction machine.

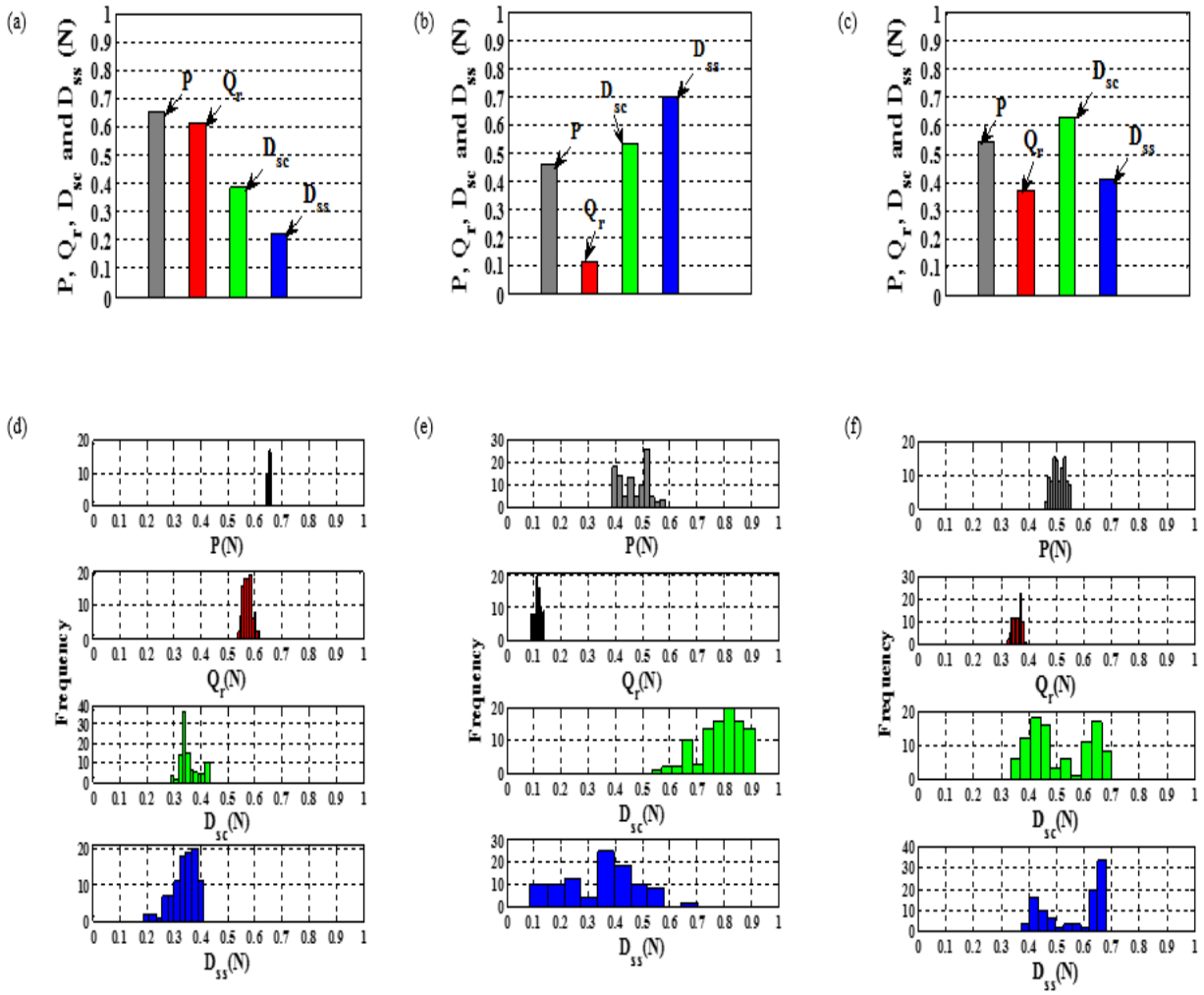

Figure 9. The normalised values of P, Q_r, D_{sc} and D_{ss} measured under sinusoidal supply voltage for (a) a dimmer controlled R-L impedance, (b) a number of computers and (c) a number of compact fluorescent lamps, and the histograms of the normalised powers measured under distorted test voltages for (d) a dimmer controlled R-L impedance, (e) a number of computers and (f) a number of compact fluorescent lamps.

On the other hand, it can be mentioned from Figure 8 (b), (c), (e) and (f) that the constant torque and constant speed cases of the induction machine have almost the same power values for sinusoidal and the distorted test voltages.

It is seen from Figure 9 (a) that P, Q_r, D_{sc} and D_{ss} of the R-L impedance controlled with a dimming circuit are 0.65, 0.61, 0.38 and 0.23 pu for sinusoidal supply voltage. Figure 9 (a) and (d) show that the P values drawn by the same load under sinusoidal and the distorted test voltages are very close. In addition to that, for the distorted test voltages, Q_r, D_{sc} and D_{ss} vary in the intervals from 0.5 to 0.6 pu, from 0.3 to 0.4 pu and from 0.2 to 0.4 pu, respectively.

It is observed from Figure 9 (b) that P, Q_r, D_{sc} and D_{ss} of the computers are 0.45, 0.11, 0.53 and 0.70 pu for sinusoidal supply voltage. Figure 9 (b) and (e) shows that the Q_r values drawn by the same load under sinusoidal and the distorted test voltages are very close. For the distorted test voltages, P, D_{sc} and D_{ss} vary in the intervals from 0.4 to 0.6 pu, from 0.5 to 0.9 pu and from 0.1 to 0.7 pu, respectively

It can be mentioned from Figure 9 (c) that the P, Q_r, D_{sc} and D_{ss} of the compact fluorescent lamps are measured as 0.54, 0.37, 0.63 and 0.41 pu in sinusoidal supply voltage case. For the distorted test voltage cases, the histograms plotted in Figure 9 (f) show that P is in the interval between 0.4 and 0.6 pu, Q_r is in the interval between 0.3 and 0.4 pu, D_{sc} is in the interval between 0.3 and 0.7 pu, and D_{ss} is in the interval between 0.3 and 0.7 pu.

From statistical results given above, one can see that D_{sc} could be successfully used to detect harmonic producing loads under sinusoidal and distorted supply voltages due to the fact that it has two distinct cases for the linear and nonlinear (harmonic producing) loads:

- The normalised values of D_{sc} measured for R-L impedance and induction machine are almost zero.
- However, for the harmonic producing loads, D_{sc} has large normalised values.

5. Conclusions

In this paper, a power resolution is proposed for unbalanced and nonsinusoidal systems. The motivation of the proposed resolution is to provide the direct determination of the power of optimum balanced capacitive compensator and to be used for detection of the harmonic producing loads in the smart power grids.

The simulation studies and analytical expressions show that the resolution achieves its compensation goal for the systems. In addition to that, the results demonstrated that it can practically be employed as a tool to design the cost effective unity power factor compensator consisting of the basic capacitors and an active compensator.

On the other hand, the scattered conductance power (D_{sc}) of the proposed resolution is statistically investigated for various load types and supply voltages in an experimental test system. Consequently, it is observed from the results that the normalised value of this power component is very close to zero for linear loads and it has considerably high value for nonlinear (harmonic producing) loads. Thus, it is pointed out that in the smart power grids harmonic producing loads could be detected by using the proposed resolution implemented in the demand meters.

Finally, due to fact that all power components of the proposed power resolution are related to the load conductance and susceptance parameters, it may provide a collective operation platform including not only the basic capacitors & active compensators, demonstrated as in this paper, but also other types of compensators. This will be studied in a future work.

6. References

[1] M. E. Balci, M. H. Hocaoglu, "A power resolution for nonsinusoidal and unbalanced systems — Part I: Literature overview and motivation", *ELECO 2011*, Bursa, Turkey, 1-4 December 2011, pp. I-167 - I-172.

[2] M. E. Balci, A. E. Emanuel, "Apparent power definitions: A comparison study", *IREE Journal*, vol. 6, no. 6, pp. 2713-2722, November 2011.

[3] M. E. Balci, M. H. Hocaoglu, "Quantitative comparison of power decompositions", *Electric Power Systems Research*, vol. 78, no. 3, pp. 318-329, March 2008.

[4] M. E. Balci, M. H. Hocaoglu, "Comparative review of multi-phase apparent power definitions", *ELECO 2009*, Bursa, Turkey, 5-8 November 2009, pp.I-144,I-148.

[5] M. E. Balci, M. H. Hocaoglu, "A current decomposition-based method for computationally efficient implementation of power resolution meters in non- sinusoidal single-phase systems", *Metrology and Measurement Systems*, vol. 20, no. 2, pp. 263-274, June 2013.

[6] M. E. Balci, M. H. Hocaoglu, ''New power decomposition for sinusoidal and nonsinusoidal conditions'', *IEEE ICHQP 2006*, Cascais, Portugal, September 2006.

[7] M. E. Hocaoglu, M. H. Hocaoglu, "An analysis on the nonactive powers for nonsinusoidal conditions", *Journal of the Faculty of Engineering and Architecture of Gazi University*, vol. 26, no. 2, pp. 307-313, June 2011 (in Turkish).

[8] M. E. Balci, M. H. Hocaoglu, "A power resolution for nonsinusoidal and unbalanced systems — Part II: Theoretical backgorund", *ELECO 2011*, Bursa, Turkey, 1-4 December 2011, pp. I-173 - I-178.

[9] M. E. Balci, M. H. Hocaoglu, "Addendum to a power resolution for nonsinusoidal and unbalanced systems: Evaluation examples", *ELECO 2011*, Bursa, Turkey, 1-4 December 2011, pp. I-179 - I-182.

[10] *AC Quantities- Part 1: Single-Phase Circuits, Part 2: Polyphase Circuits*, DIN Std. 40110, 1994 and 2002. (in German).

[11] *IEEE Standard Definitions for the Measurement of Electric Power Quantities under Sinusoidal, Non-sinusoidal, Balanced or Unbalanced Conditions*, IEEE Std. 1459, 2010.

[12] J. L. Willems, J. A. Ghijselen, A. E. Emanuel, ''The apparent power concept and the IEEE Standard 1459-2000'', *IEEE Trans. on Power Deliv.*, vol. 20, no. 2, pp. 876-884, April 2005.

[13] J. L. Willems, J. A. Ghijselen, A. E. Emanuel, ''Addendum to the apparent power concept and the

IEEE Standard 1459-2000'', *IEEE Trans. on Power Deliv*., vol. 20, no. 2, pp. 885-886, April 2005.
[14] L. S. Czarnecki, ''Physical reasons of currents RMS value increase in power systems with nonsinusoidal voltage'', *IEEE Trans. on Power. Deliv*., vol. 8, no. 1, pp. 437-447, January 1993.
[15] L. S. Czarnecki, ''Orthogonal decomposition of the currents in a 3-phase nonlinear asymmetrical circuit with a nonsinusoidal voltage source'', *IEEE Trans. on Instrum. and Meas*., vol. 37, no. 1, pp. 30-34, March 1988.
[16] H. Akagi, E. H. Watanabe, M. Aredes, "Instantaneous Power Theory and Applications to Power Conditioning", IEEE Press, John Wiley & Sons, 2007.
[17] *IEEE Recommended Practices and Requirements for Harmonic Control in Electrical Power Systems*, IEEE Std. 519, 2014.

7. Acknowledgement

This work was supported by Turkish Scientific Research Council (TUBITAK) under the project number 110E113.

Murat Erhan Balci received B.Sc. degree from Kocaeli University, M.Sc. and Ph.D. degrees from Gebze Institute of Technology, Turkey in 2001, 2004 and 2009, respectively. During 2008, he was a visiting scholar at Worcester Polytechnic Institute, USA. Since 2009, he has been with the Electrical and Electronics Engineering Department of Balikesir University, Turkey. He is, currently, an Associate Professor at the same University. He is working in the field of electric machines, power electronics, power quality, power system analysis and wind power.

Mehmet Hakan Hocaoglu received the B.Sc. and M.Sc. degrees from Marmara University, Turkey. He obtained the Ph.D. degree in 1999 from Cardiff School of Engineering, UK. From 1988 to 1993, he worked at Gaziantep University, Turkey as a Lecturer. Since 1999, he has been with the Electronics Engineering Department of Gebze Technical University, Turkey . He is, currently, a full Professor at the same University.